NASA TECHNICAL NOTE

NASA TN D-2082

AN EXAMINATION OF THE ROLLING-CONTACT FATIGUE PROCESS IN A CRYSTALLIZED-GLASS CERAMIC

by Shelley Harrell and Erwin V. Zaretsky

Lewis Research Center
Cleveland, Ohio

NATIONAL AERONAUTICS AND SPACE ADMINISTRATION • WASHINGTON, D. C. • DECEMBER 1963

TECHNICAL NOTE D-2082

AN EXAMINATION OF THE ROLLING-CONTACT FATIGUE PROCESS IN A CRYSTALLIZED-GLASS CERAMIC

By Shelley Harrell and Erwin V. Zaretsky

Lewis Research Center
Cleveland, Ohio

NATIONAL AERONAUTICS AND SPACE ADMINISTRATION

AN EXAMINATION OF THE ROLLING-CONTACT FATIGUE PROCESS IN A CRYSTALLIZED-GLASS CERAMIC

By Shelley Harrell and Erwin V. Zaretsky

SUMMARY

The NASA five-ball fatigue tester was used to stress in rolling contact 1/2-inch-diameter balls of a crystallized-glass ceramic for durations up to $1\frac{1}{4}$ million stress cycles. Standard operating conditions were room temperature and a maximum Hertz stress of 295,000 psi. The test specimens were subsequently sectioned and studied to various depths below the stressed running track by means of electron and light microscopy techniques.

In the early stages of fatigue, small holes developed in the subsurface of the stressed running track. The matrix around these holes no longer resembled the matrix of an unstressed ball specimen. As the running time increased, electron microscopy showed a series of short, disconnected, thin cracks developing in the region of these small holes. These cracks approached but stopped at the crystals in the matrix; they did not break the crystals, but worked their way around them.

Cracks normal to the surface developed independently of the subsurface cracks. Spalling or complete failure was not necessarily simultaneous with the development of surface cracks or with the subsurface-originating cracks reaching the surface. Spalling was dependent on the subsurface cracks forming a network and the subsequent degeneration of the area between the original subsurface cracks and the stressed surface of the specimen.

INTRODUCTION

With the advent of the jet age and subsequently the space age, bearing technology has become more complex because of high load and temperature requirements. New materials have been developed to meet these requirements. High reliability has become of paramount importance. However, to assure the required reliability in these new bearing materials, it is necessary that the rolling-contact fatigue phenomenon be understood.

Among the new materials considered for high-temperature application is a crystallized-glass ceramic known commercially as Pyroceram 9608. Research on rolling-contact fatigue at the NASA Lewis Research Center (refs. 1 and 2) indicates that the failed or spalled area in this material is limited in area and

depth of penetration, and there are indications of a stress-affected zone in the subsurface region of the running track. These failures appear similar to those of steels.

In view of the aforementioned, a study of the rolling-contact fatigue process in this crystallized ceramic may give an insight into the fatigue phenomenon in other types of high-temperature material. Therefore, the objectives of the research contained herein were (1) to investigate the fatigue phenomenon in Pyroceram 9608 and (2) to determine the mechanism of development for incipient fatigue cracks and the manner of their propagation. To accomplish these objectives, light and electron microscopy methods developed at the NASA Lewis Research Center (ref. 3) were employed to study Pyroceram ball specimens, each with a running track that had been stressed in rolling contact for various lengths of time, up to $1\frac{1}{4}$ million stress cycles.

BACKGROUND

There appears to be no reported literature pertaining to a basic study of the rolling-contact fatigue phenomenon of a crystallized-glass ceramic. However, it is reported in references 1 and 2 that there is some similarity in the fatigue appearance of Pyroceram 9608 and bearing steels. Therefore, even though the structure of these two types of materials may be dissimilar, it was believed that a review of the literature reporting findings pertaining to the rolling-contact fatigue phenomenon of bearing steels might give some insight into the fatigue process of a crystallized-glass ceramic such as Pyroceram 9608.

An early theory of rolling-contact fatigue is advanced in reference 4. Here it is theorized that microscopic cracks originally located on the surface of a steel rolling element are propagated into fatigue spalls (failures) by the lubricating fluid penetrating these cracks under contact pressure. However, evidence obtained with radially loaded, grooved ball bearings, stressed to a maximum Hertz stress of 800,000 psi on the inner race, indicates that fatigue cracking (and subsequent spalling) begins below the surface of the stressed race (ref. 5). This same observation was also reported in references 6 and 7. In these references it was noted that the incipient cracks appear to initiate at inclusions or other (material) defects in the subsurface region of resolved shear stress. A more extensive study reported in reference 8 not only substantiated these observations but pinpointed the type of inclusions detrimental to bearing fatigue life. These inclusions were believed to act as stress raisers, analogous to notches in tension-compression and rotating-beam specimens. The cracks emanating from these inclusions appeared to propagate to the specimen surface to form a spall or failure, which was limited in area and depth of penetration. (The spalled area had a diameter roughly equal to that of the running track width, and the depth extended approximately to the depth of the maximum shearing stress.) From the studies of references 5 to 8 it might be postulated that bearing steels with fewer inclusions would generally give longer lives. However, research undertaken to determine the effect of material cleanliness produced by different material fabrication processes and reported in references 9 and 10 indicates that improved fatigue life of bearings made of vacuum-melted steels does not appear to be commensurate with the improvement in cleanliness.

Bearing steels in general have a martensitic structure, which appears to undergo a transformation to tempered martensite in the subsurface zone of resolved shear stress because of continued stress cycling. This phenomenon was reported in references 5 to 8 and 11. It was suggested in the discussion to reference 11 that this change might not be a change to tempered martensite but is in essence a work hardening. If this be the case, the same phenomenon may then occur in nonferrous materials such as Pyroceram.

MATERIALS AND APPARATUS

Pyroceram

Pyroceram is essentially a glass to which a nucleating agent, usually titanium dioxide, has been added. It obtains its special qualities only after two heat-treating processes. Because all the material is not converted into crystals in this process, the final product is a crystallized phase in an amorphous matrix.

Before heat treating, Pyroceram 9608 was cast into raw spherical blanks approximately 3/4 inch in diameter. After heat treating, the raw blanks were ground to finished 1/2-inch-diameter balls.

Because the chemistry of glasses is similar to that of crystallized-glass ceramics, the structural differences between these types of materials should be pointed out. Photomicrographs of two representative glass products and two types of Pyroceram are shown in figure 1 for comparative purposes. Figure 1(a) is sheet glass (window glass) and has no appreciable structure that can be seen. A second type of glass, Carrara glass (fig. 1(b)), has a rather heterogeneous structure with no particular concentration or orientation of the crystals. The structures of these glasses can be compared with the structures of the two crystallized-glass ceramics in figures 1(c) and (d). Figure 1(c) shows Pyroceram 9606, which has a structure of very large crystals randomly oriented and closely spaced together in an amorphous matrix. As can be seen from this electron micrograph, it is difficult to distinguish the smaller crystals from the matrix. The structure of the other crystallized-glass ceramic, Pyroceram 9608, is shown in figure 1(d). Pyroceram 9608 differs from the two glasses and Pyroceram 9606 in that its crystals are small, somewhat evenly dispersed, and randomly oriented within the amorphous matrix. Therefore, fatigue cracks in this material can be detected with relative ease.

Test and Related Equipment

The NASA five-ball fatigue tester shown in figure 2 was used to stress the Pyroceram 9608 test specimens in rolling contact. Essentially, this fatigue apparatus consists of a 1/2-inch-diameter test specimen (Pyroceram ball) pyramided upon four lower 1/2-inch-diameter support balls (M-1 steel balls), which are positioned by a separator and are free to rotate in an angular-contact raceway (fig. 2(b)).

The ball specimen is analogous in operation to the inner race of a ball

bearing, while the support balls and the angular-contact raceway are analogous to the balls and the outer race of a ball bearing, respectively.

For every revolution of the drive shaft, the test specimen receives three stress cycles. This type of fatigue tester produces the spalls and the incipient cracks in the running track of a ball specimen being studied. A more detailed description of this apparatus is given in reference 1.

Standard light and electron microscopy equipment were used to obtain the results reported herein.

PROCEDURE

Sixteen 1/2-inch ball specimens of Pyroceram 9608 were run in the NASA five-ball fatigue tester for durations up to $1\frac{1}{4}$ million stress cycles at 7080 stress cycles per minute. The fatigue tests were run at room temperature (no heat added) with a synthetic diester lubricant meeting the MIL-L-7808C specification. The ball load was selected to produce a maximum Hertz stress of 295,000 psi.

Subsequent to being run in the fatigue tester, the specimens were mounted in lucite so that the track orientation could be seen. Two specimen orientations were adopted. In the first, the specimen was positioned in the mount so that a radial line extending from the center of the ball to a fully developed spall or fatigue failure in the ball running track was perpendicular to the polishing surface (fig. 3(a)). The other specimen orientation is shown in figure 3(b). Here the plane of the running track is parallel to the polishing surface. The advantage of orienting the ball specimen as in figure 3(a) would be to study the fatigue cracks emanating from the spalled or failed area, propagating parallel and below the running track. If the specimen is oriented as in figure 3(b), the incipient cracks are seen in longitudinal section and can be readily located without the specimen having spalled.

Once mounted in lucite, the specimens were ground and polished through the running track a few microns at a time. The exposed surface was examined by light and electron microscopy (by the methods described in ref. 3) for changes in the material.

The most satisfactory etching process used for the Pyroceram specimens consisted of a primary etchant of 5 parts of hydrochloric acid (concentrated), 5 parts of hydrofluoric acid (45 percent), and 45 parts of water, then a secondary etchant with methyl alcohol instead of the water. Best results were obtained with total etching time ranging from 25 to 30 seconds.

A replication technique was employed for the specimens that makes use of preshadowed silicon monoxide replicas deposited after the application of a dehydrated liquid detergent releasing agent (ref. 3). This procedure eliminated the difficulties encountered with plastic replicas because of their tendency to adhere to the specimen and to tear when removed.

Subsequent to each examination of the specimen surface, the surface was

ground a few additional microns and reexamined. The length and position (surface or subsurface) of each incipient crack observed were recorded, and in the case of subsurface cracks the range of depths below the surface was also recorded.

DISCUSSION OF RESULTS

Surface Cracks

Two unstressed specimens were ground, mounted, polished, and examined in order to have a basis for comparing those specimens that had been stressed. Before sectioning, these unstressed specimens appeared to be perfectly sound and flawless under reflected-light microscopy examination. However, when they were sectioned, it was noticed that the unstressed specimens had small cracks originating at the surface. These surface cracks ranged in length to as much as 0.003 inch. Figure 4 is a representative micrograph of a surface crack originating in an unstressed ball. (It is believed that these surface cracks are initially caused by the high friction forces induced in the grinding process used in finishing the balls. No better finishing process is presently available. However, it has been shown in reference 12 that small cracks are inherent in the surface of some glass products and appear to be of the same magnitude as those observed on the surface of the Pyroceram specimens.) As the ball specimens were stressed in rolling contact, the number of surface cracks increased. The average number of surface cracks around a stressed track for given running times and their range of lengths are given in table I.

Subsurface Cracks

Examination of unstressed specimens with electron microscopy revealed no subsurface material defects. However, examination of all the specimens stressed by electron microscopy revealed small "holes" in the subsurface region even when no crack was optically visible. The electron micrograph in figure 5 shows that the matrix around these holes no longer resembles the matrix of an unstressed ball (cf. fig. 1(d)). It is not known what changes took place in the matrix that lead to the formation of the holes and their growth to the size shown in figure 5. As the running time of the specimen became greater, electron microscopy showed a series of short, disconnected, thin cracks that appeared to emanate from the holes in the subsurface matrix (fig. 6).

As the specimen was continually stressed, these small cracks that appeared to emanate from the holes joined to form larger cracks which were observable as shown in the electron micrograph in figure 7. These cracks approached but stopped at the crystals, then they detoured around them. In figure 7, the crack has completely propagated around crystal X, which is perpendicular to the plane of the micrograph, leaving a dark area in the picture. At crystal Y, which is parallel to the plane of the micrograph, the crack widens into a dark area on either side of the crystal. Careful examination of many specimens revealed that the crystals themselves were intact and that the widest dark portion of the crack was where the crack had grown around them.

The subsurface incipient cracks initially propagated parallel to the surface

of the running track. The subsurface cracks joined and formed a three-dimensional network (fig. 8) and, as such, worked their way to the surface after repeated stressing. Because the crack network did not engulf the entire volume of a potential spalled area, failure was not simultaneous with the crack network reaching the surface. However, the unfractured material was structurally weakened and crumbled, as evidenced by a multiple layer of cracks between the surface and what appeared to be the original crack network. This crumbled volume subsequently flaked off as multiple minute pieces to form a spall or fatigue failure. Data for subsurface developed cracks are also given in table I.

In references 1 and 2 it was noted that several spalls occurred around the race of Pyroceram ball specimens at about the same number of stress cycles. In the investigation herein it was observed that subsurface incipient cracks also developed at about the same time at different locations around the running track or race. This occurred because the material as a whole has a relatively uniform microstructure in that the crystallites are rather evenly dispersed throughout the structure, which makes the probability of crack formation and development into a spall approximately equal for all stressed sections of the ball specimen.

In the course of examining the stressed specimens, there appeared to be indications that the frequency of cracking was lowest and that the cracks were shortest where the crystals were most closely spaced. This could occur for two reasons. First, the crystals themselves would tend to block the formation of longer cracks by inhibiting the propagation of the crack, as mentioned previously. Second, the crystals could effectively strengthen the zone more than if they were widely separated, thereby retarding the initiation of the crack. Thus, the rate of formation of cracks as well as the crack propagation rate could be related to the spacing between the crystals.

GENERAL COMMENT

As indicated previously, the fatigue phenomena of a bearing steel and of a crystallized-glass ceramic may have parallels. For Pyroceram 9608, it is suggested that fatigue cracks initiate at small holes induced by repeated stresses on the ball specimen. Polycrystalline, ionic compounds, and even amorphous ceramics probably have defects randomly distributed in the structure. Presumably such defects may be created by the presence of impurities or by thermal or mechanical stressing of the materials. Thus, cyclic stressing accompanying the testing of the bearings could very readily cause defects to form in those areas where stresses are concentrated (e.g., in the area of the resolved shear stress that occurs below the surfaces of bearings).

In bearing steels it is probable that vacancies or voids exist in the grain boundaries prior to stressing. Also, it would be expected that the martensitic needles that make up the grain of the steel not only intersect but also produce stress concentrations that could furnish sites almost at random locations.

The basic differences between an amorphous-glass matrix such as that found in Pyroceram (that could contain random vacancy sites) and a fine martensitic structure (that on an overall basis should have almost a random distribution of vacancy sites) may not be so great that behavior analogies should not be drawn

between the two types of materials. Other similarities between the two materials are their extreme hardness and the fact that bearing steels and Pyroceram have dispersed phases throughout the microstructure.

SUMMARY OF RESULTS

Electron and light microscopy techniques were used to study the rolling-contact fatigue characteristics of a crystallized-glass ceramic known commercially as Pyroceram 9608. The structure of 1/2-inch-diameter ball specimens of this material stressed in rolling contact for various lengths of time (up to 1.25×10^6 stress cycles) was studied at various depths below the surface. The following are the results and conclusions of this study:

1. Prior to stressing the ball specimens, surface microcracks were detected by light and electron microscopy. The origin of these cracks can presumably be found in the grinding process used in finishing the ball specimens.

2. Surface cracks were found to increase in number and length with increasing stress cycles.

3. Subsurface cracks were found to develop upon stress cycling. The sequence of events leading to the formation of subsurface cracks is believed to be as follows:

   a. Holes develop in the subsurface zone of resolved shear stress because of changes caused by cyclic stressing.

   b. A crack initiates in the disturbed zone coincident with a hole, presumably at the hole itself. The cracks propagate through the amorphous matrix until they reach a dispersed crystal at which point they deviate around the crystal.

4. Subsurface cracks propagate to the surface and also connect with surface cracks to form a network. The volume enclosed by this network crumbles, thus producing a spall or fatigue failure.

Lewis Research Center
National Aeronautics and Space Administration
Cleveland, Ohio, August 14, 1963

REFERENCES

1. Carter, Thomas L., and Zaretsky, Erwin V.: Rolling-Contact Fatigue Life of a Crystallized Glass Ceramic. NASA TN D-259, 1960.

2. Zaretsky, E. V., and Anderson, W. J.: Rolling-Contact Fatigue Studies with Four Tool Steels and a Crystallized Glass Ceramic. Jour. Basic Eng. (ASME Trans.), ser. D, vol. 83, no. 4, Dec. 1961, pp. 603-612.

3. Harrell, Shelley, and Zaretsky, Erwin V.: Electron and Light Microscopy Techniques Suitable for Studying Fatigue Damage in a Crystallized Glass Ceramic. NASA TN D-1161, 1961.

4. Way, Stewart: Pitting Due to Rolling Contact. Jour. Appl. Mech., vol. 2, no. 1, June 1935, pp. A49-A58; discussion, pp. A110-A114.

5. Jones, A. B.: Metallographic Observations of Ball Bearing Fatigue Phenomena. Symposium on Testing of Bearings, ASTM, 1947, pp. 35-52; discussion, pp. 49-52.

6. Bear, H. Robert, and Butler, R. H.: Preliminary Metallographic Studies of Ball Fatigue Under Rolling-Contact Conditions. NACA TN 3925, 1957.

7. Carter, T. L., Butler, R. H., Bear, H. R., and Anderson, W. J.: Investigation of Factors Governing Fatigue Life with the Rolling-Contact Fatigue Spin Rig. ASLE Trans., vol. 1, no. 1, Apr. 1958, pp. 23-32.

8. Johnson, R. F., and Sewell, J. F.: The Bearing Properties of 1 Percent C-Cr Steel as Influenced by Steelmaking Practice. Jour. Iron and Steel Inst., pt. 4, vol. 196, Sept.-Dec. 1960, pp. 414-444.

9. Morrison, T. W., Walp, H. O., and Remorenko, R. P.: Materials in Rolling-Element Bearings for Normal and Elevated (450° F) Temperatures. ASLE Trans., vol. 2, no. 1, Apr. 1959, pp. 129-146.

10. Jackson, E. G.: Rolling-Contact Fatigue Evaluation of Bearing Materials and Lubricants. ASLE Trans., vol. 2, no. 1, Apr. 1959, pp. 121-128.

11. Bush, J. J., Grube, W. L., and Robinson, G. H.: Microstructural and Residual Stress Changes in Hardened Steel Due to Rolling Contact. Trans. ASM, vol. 54, no. 3, Sept. 1961, pp. 390-412; discussion, pp. 818-824.

12. Anderson, O. L.: The Griffith Criterion for Glass Fracture. Fracture, B. L. Averbach, D. K. Felbeck, G. T. Hahn, and D. A. Thomas, eds., The Tech. Press, M.I.T., 1959, p. 347.

TABLE I. - CRACK ORIGIN AND PROPAGATION FOR PYROCERAM 9608 TESTED AT 295,000-PSI MAXIMUM HERTZ STRESS AND 2360 RPM IN THE NASA FIVE-BALL FATIGUE TESTER

Time, stress cycles	Surface cracks		Subsurface cracks		
	Range of length, in.$\times 10^3$	Approximate number	Range of depth, in.$\times 10^3$	Range of length, in.$\times 10^3$	Approximate number
0	-------	3	--------	---------	0
113×10^3	3.4-9.9	6	4.9-21.0	19.2-35.0	5
339	8.4-10.4	10	3.5-38.6	6.9-80.4	8
566	8.4-31.2	12	4.9-25.4	6.9-43.6	[a]16
1218	8.3-43.0	15	(b)	(b)	(b)

[a]Cracks of subsurface origin can no longer be clearly distinguished from those of surface origin.

[b]Fully developed spall or failure.

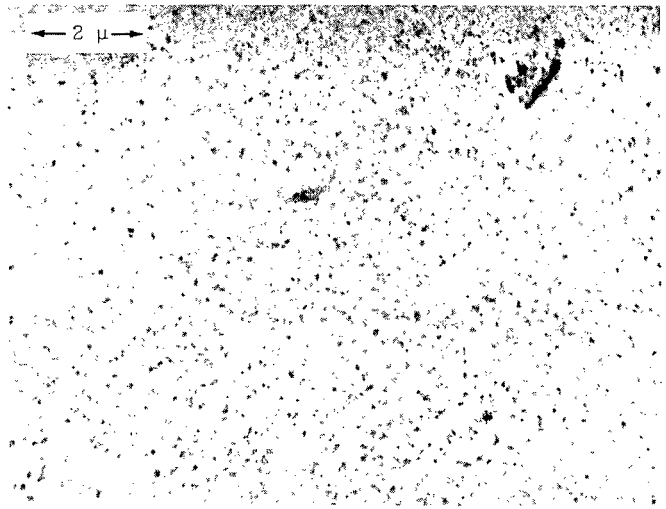

(a) Window glass.

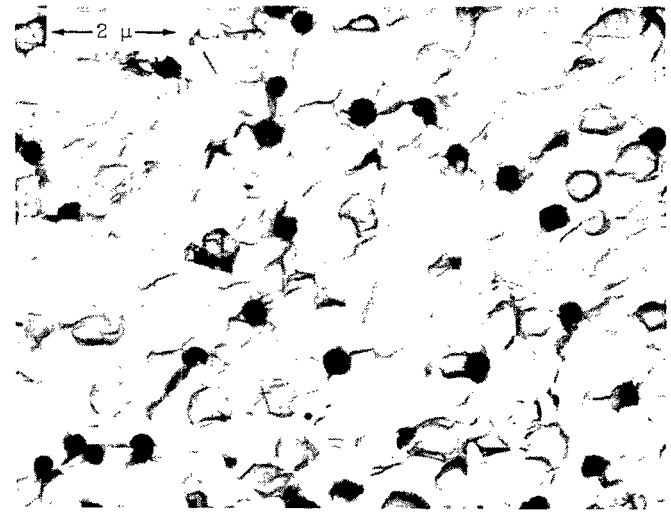

(b) Carrara.

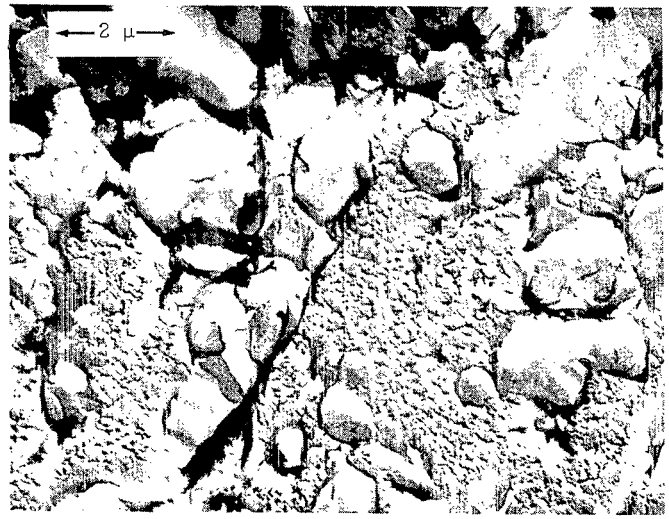

(c) Pyroceram 9606.

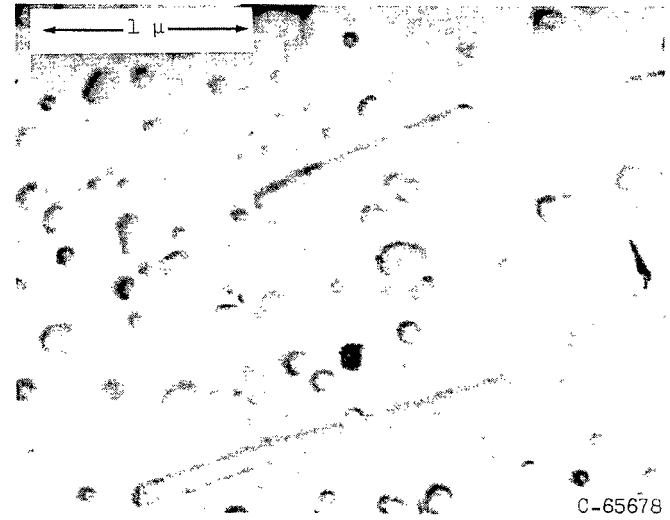

(d) Pyroceram 9608.

Figure 1. - All samples etched with a solution of hydrofluoric acid, hydrochloric acid, and water for 15 seconds and then a solution of hydrofluoric acid, hydrochloric acid, and alcohol for 10 seconds (electron micrographs). Rotary shadowed with chromium at approximately 30°.

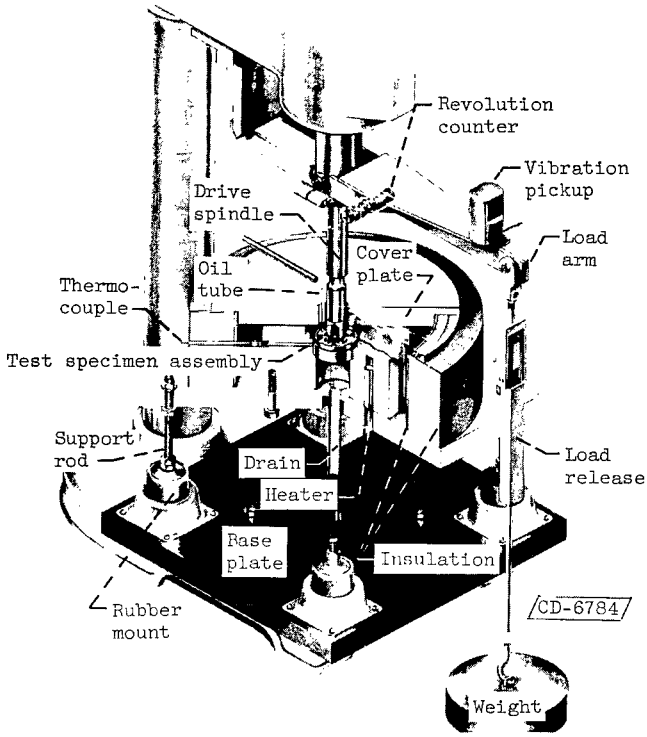

(a) Isometric view.

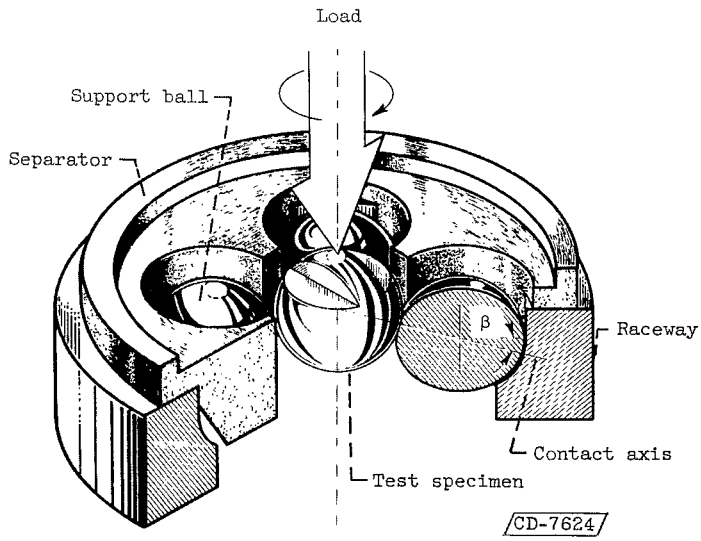

(b) Schematic diagram.

Figure 2. - Five-ball fatigue tester.

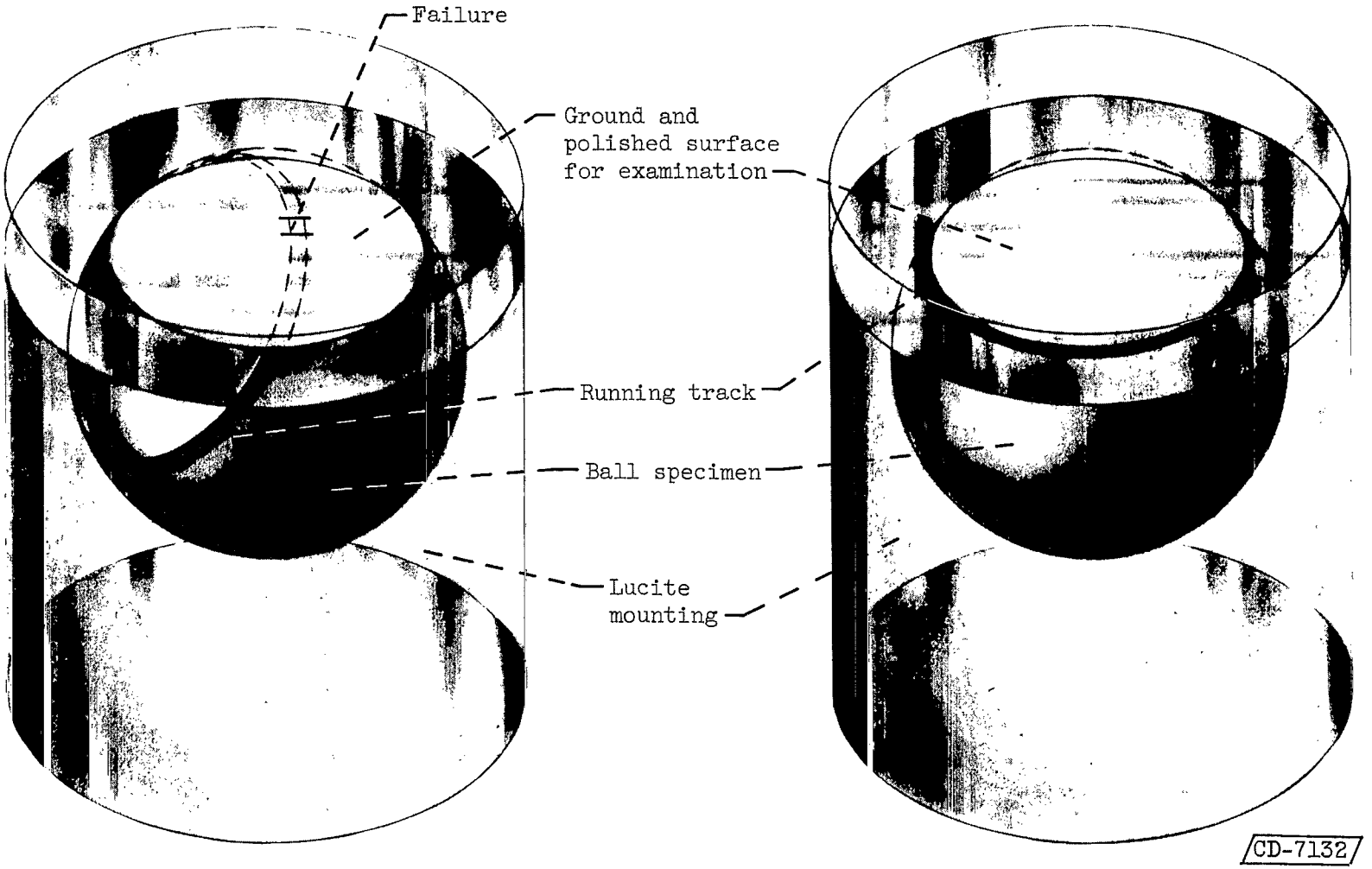

(a) Radius to failure in track perpendicular to polishing surface.

(b) Plane of running track parallel to polishing surface.

Figure 3. - Mounting of ball specimen for examination under light and electron microscopy.

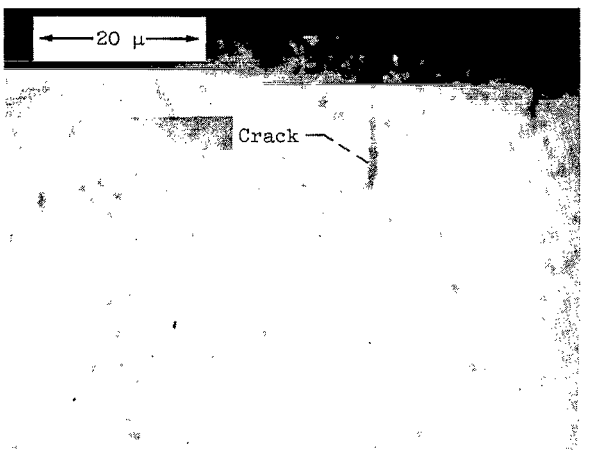

Figure 4. - Cross section of crack of surface of an unstressed ball (light micrograph). Etchant: solution of hydrofluoric acid, hydrochloric acid, and water for 15 seconds; solution of hydrofluoric acid, hydrochloric acid, and alcohol for 10 seconds. Stained with Sanford's marker (red).

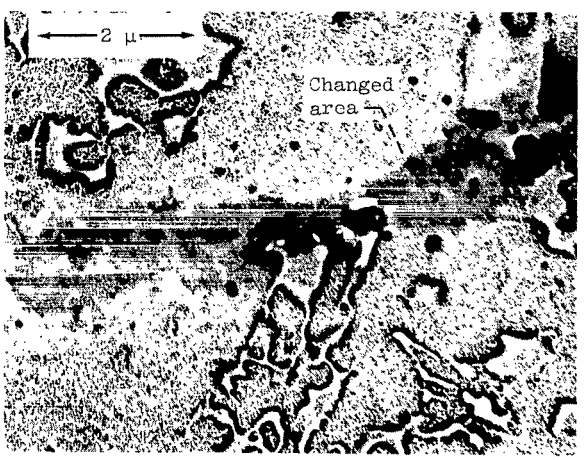

Figure 5. - Subsurface showing "holes" and region of change in the matrix (electron micrograph). Etchant: solution of hydrofluoric acid, hydrochloric acid, and water for 10 seconds; solution of hydrofluoric acid, hydrochloric acid, and alcohol for 30 seconds. Rotary shadowed heavily with chromium at approximately 30°.

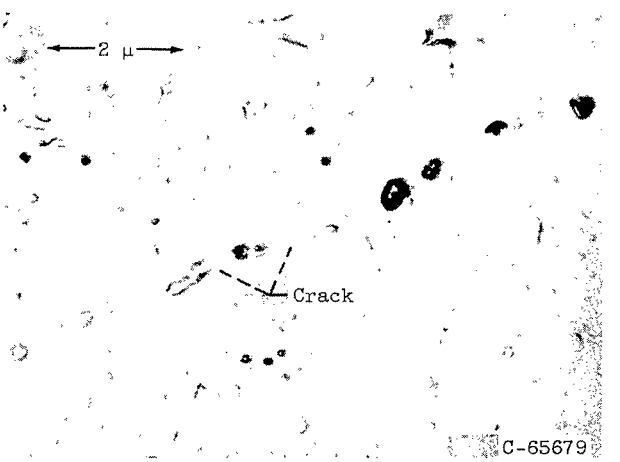

Figure 6. - Subsurface showing short cracks that have not yet connected (electron micrograph). Etchant: solution of hydrofluoric acid, hydrochloric acid, and water for 15 seconds; solution of hydrofluoric acid, hydrochloric acid, and alcohol for 5 seconds. Rotary shadowed with chromium at approximately 30°

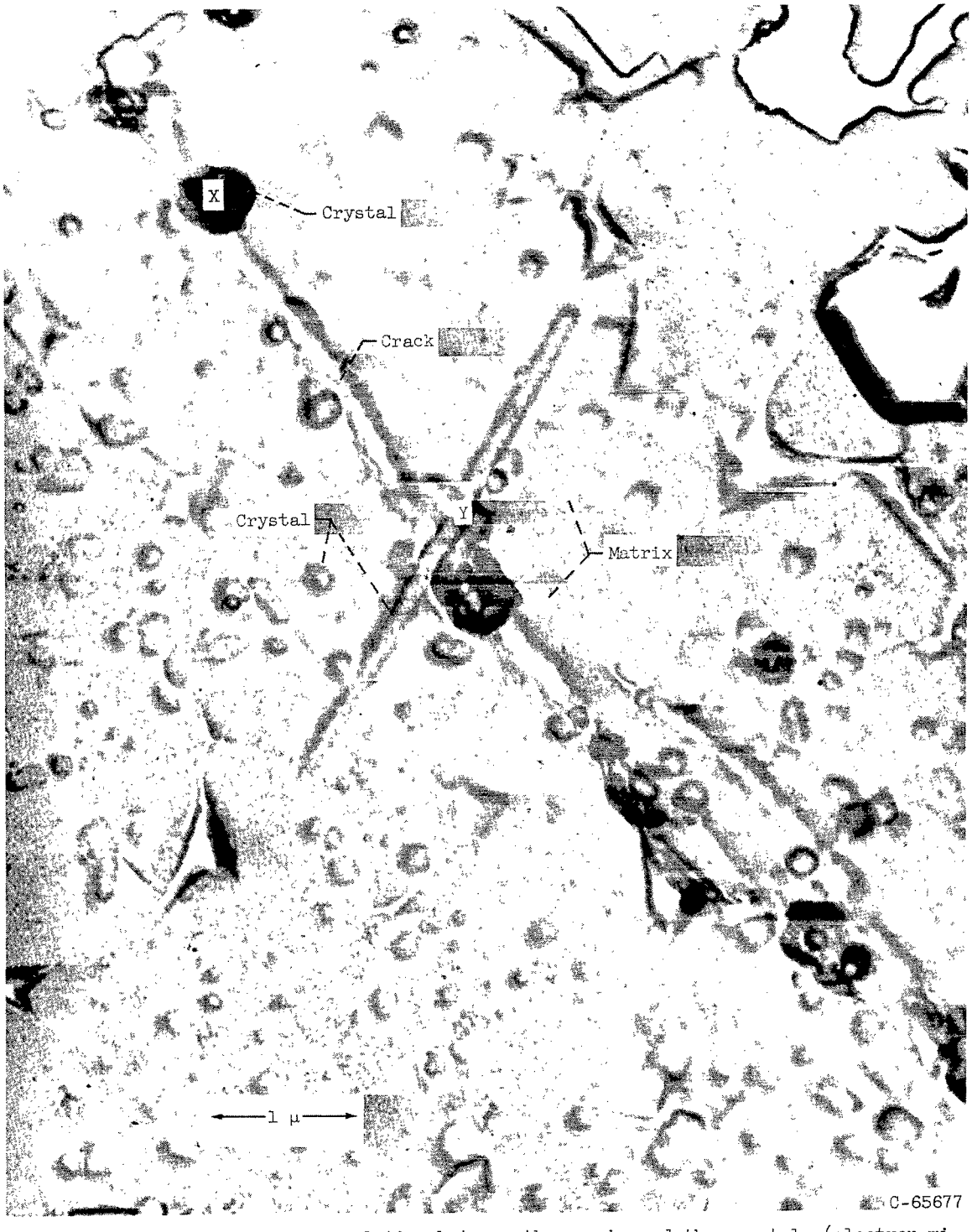

Figure 7. - Subsurface showing relation between the cracks and the crystals (electron micrograph). Neither crystal X, which is perpendicular to the plane of the micrograph, nor crystal Y, which is parallel, can be seen to be broken by the progression of the crack. Etchant: solution of hydrofluoric acid, hydrochloric acid, and water for 15 seconds; solution of hydrofluoric acid, hydrochloric acid, and alcohol for 10 seconds. Rotary shadowed with chromium at approximately 30°.

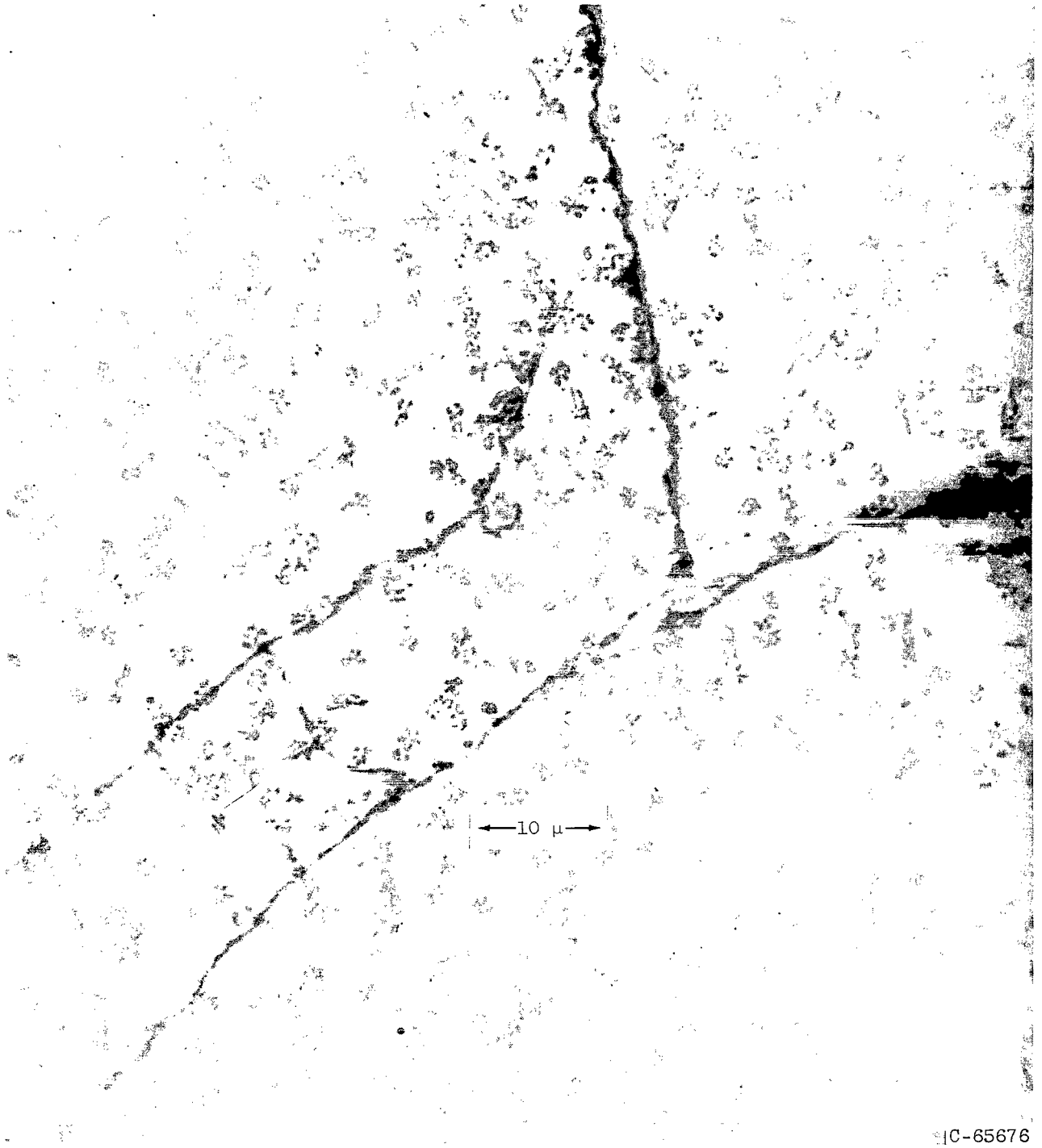

C-65676

Figure 8. - Subsurface showing a network of cracks that has developed (light micrograph). Etchant: solution of hydrofluoric acid, hydrochloric acid, and water for 20 seconds; solution of hydrofluoric acid, hydrochloric acid, and alcohol for 5 seconds. Stained with Sanford's marker (red).